NANO LETTERS

2008
Vol. 8, No. 1
42−48

Electroosmotic Flow in Nanotubes with High Surface Charge Densities

Yunfei Chen,* Zhonghua Ni, and Guiming Wang

School of Mechanical Engineering and China Education Council Key Laboratory of MEMS, Southeast University, Nanjing, 210096, People's Republic of China

Dongyan Xu and Deyu Li

Department of Mechanical Engineering, Vanderbilt University, Nashville, Tennessee 37235-1592

Received July 30, 2007; Revised Manuscript Received November 13, 2007

ABSTRACT

The ion distribution and electroosmotic flow of sodium chlorine solutions confined in cylindrical nanotubes with high surface charge densities are studied with molecular dynamics (MD). To obtain a more practical physical model for electroosmotic driven flow in a nanoscale tube, the MD simulation process consists of two steps. The first step is used to equilibrate the system and to obtain a more realistic ion distribution in the solution under different surface charge densities. Then, an external electric field is acted to drive the liquids. The simulation results indicate that with the increase of the surface charge density, both the thickness of the electric double layer and the peak height of the counterion density increase. However, the phenomenon of charge inversion does not occur even as the surface charge density increases to −0.34 C/m^2, which is rather difficult to reach for real materials in practical situations. This simulation result confirms the recent experimental observation that monovalent ions of sufficiently high concentrations can reduce or even cancel the charge inversion occurred in the case of multivalent ions [F. H. J. van der Heyden et al. *Phys. Rev. Lett.* 2006, 96, 224502].

Generally, when an electrolyte is in contact with a solid surface, the chemical state of the interface is changed, which results in a layer of surface charges. An electrical double layer (EDL) is formed as a result of the interaction between the electrolyte solution and the dielectric surface. The counterions are attracted by the surface so that they accumulate in the electrical double layer close to the surface. Electroosmotic flow is created when an external electrical field is acted on the EDL region, and the fluid will be driven by the moving ions in the diffuse layer. Electroosmotic flow has recently been utilized in various bio-M/NEMS (Micro/Nano−Electro−Mechanical−Systems) devices to transport and control liquids for different purposes, such as micropumps, chemical reactions, and species separation.[1−7] In nanofluidic systems, the channel dimensions are comparable to the thickness of electrical double layers, so the Poisson−Boltzmann (PB) and the Navier−Stokes (NS) equation, which are based on continuum assumptions, may fail to describe the ion distribution and electroosmotic flow.[8−15]

Freund[9] simulated the electroosmotic flow of 0.01 M solution of Cl^- confined in nanochannels with discrete charges and uniformly distributed charges on the surface atoms. He found in both cases the concentrations of the counterions near the wall from the molecular dynamics (MD) simulation are much higher than that predicted by the Poisson−Boltzmann theory. Qiao and Aluru[10,11] also found the discrepancies between the MD results and the continuum theory in an electrokinetic system and proposed a modified Poisson−Boltzmann equation according to the MD data. To predict the fluid flow in a larger channel, they introduced a technique to embed the velocity near the channel wall obtained from the MD simulation of electroosmotic flow in a narrow channel into the prediction for the larger ones. However, the modifications fail totally in a 0.95 nm channel because the viscosity varies significantly through the channel. Zhu and co-workers[12] corrected the ion distribution and used it as an input for the hydrodynamic theory, which agrees with the numerical simulations in nanochannels with good accuracy. However, all of these models are for two-dimensional channels and have deficiencies such as the assumption of the elementary charge distribution in which a unit charge is uniformly distributed on several wall atoms that is contradictory to the indiscrete characteristic of an elementary charge. In addition, the numbers of the counter- and co-ions in the electrolyte were assigned somewhat arbitrarily corresponding to an unknown bulk concentration. It is a common practice that the co-ion concentration is treated as the concentration of the bulk electrolyte. However, in a nanochannel when the electric double layers overlap this might not be true, and the accurate bulk concentration is unknown.

* Corresponding author. E-mail: yunfeichen@seu.edu.cn.

10.1021/nl0718566 CCC: $40.75
Published on Web 12/21/2007

The fluid−wall interactions in nanochannels have great effects on the ion distribution. Particularly, a cylindrical wall with a higher surface-to-volume ratio is expected to have a significant effect on the fluid. For example, charge inversion and flow reversal are greatly affected by the surface and the finite size effect of the ions. Charge inversion occurs when the density of co-ions exceeds that of counterions at a certain location in the EDL. Using the reference hypernetted chain approximation, Greberg and Kjellander modeled the aqueous systems with monovalent electrolytes and divalent electrolytes.[13] It was found that this phenomenon could be observed by having larger co-ions than counterions in the electrolyte with monovalent ions, while for divalent electrolytes it occurred mainly for electrostatic reasons. Their simulation results indicated that charge inversion readily occurred when the electrolyte concentration was sufficiently high. Qiao and Aluru used molecular dynamics model to investigate the cause of charge inversion in the EDL.[8] They simulated the ion distribution in sodium chloride solutions confined in two parallel slabs with negatively charged surfaces. MD simulations showed that the nonelectrostatic ion−water interactions contributed significantly to the accumulation of Na^+ ions near the wall.[8] The Cl^- ions tend to stay away from the channel wall because of the nonelectrostatic interactions among the Cl^- ions, the wall atoms, and the water molecules. The different migration directions for the two types of ions make it possible for charge inversion to occur in the double layer. When an electric field is acted in this case, charge inversion may cause flow reversal for electroosmotic driven flow.[8]

In this paper, we used a more detailed MD simulation to study the ion distribution and electroosmotic flow in smooth nanoscale cylindrical pores. The interactions between the ion−ion, ion−water, and ion−wall were calculated explicitly in the MD simulation with the Lennard-Jones potential and Coulomb potential. Here, tubes with different surface charge densities are presented with exact numbers of charges on the tube surface. The velocity profiles of the electroosmotic flow under different conditions are also given and compared with the results solved from the Poisson−Boltzmann and Navier−Stokes equations based on the continuum assumptions. Different from the previous MD models,[8,9] the model in this paper consists of three regions that include two liquid sinks on the two ends of the tube and a middle region to play as the electroosmotic pump. MD results demonstrate that with the increase of the surface-charge density, both the thickness of the electric double layer and the peak height of the counterion density increase. However, the phenomenon of charge inversion does not occur even as the surface density increases to -0.34 C/m^2. This result is different from previous MD model,[8] but, it agrees well with the recent experimental results.[26] The simulation results confirmed that the charge inversion that resulted from multivalent ions can be reduced or even canceled by monovalent ions at sufficiently high concentrations. On the basis of the MD simulation results for the nanoscale tube, different boundary conditions are introduced to solve the PB and NS equations to fit the MD results. It is confirmed that the classical equations that are based on continuum assumptions can predict the trends of the ion distribution and the flow profile with modified boundary conditions. However, it cannot be used to describe the layering structures of the liquid and ion distribution near the solid interface, where molecular interactions play great roles.

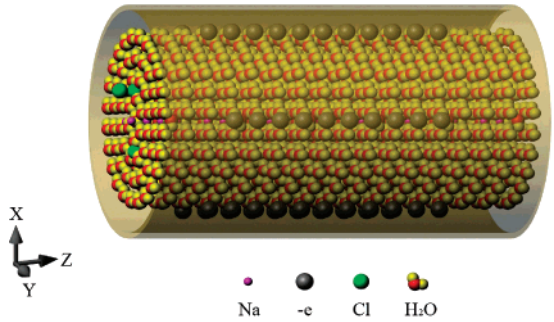

Figure 1. A schematic diagram of the nanotube model in this investigation. The original point locates at the center of the left end. Periodic boundary conditions are only applied in the z direction, which is along the axis of the cylinder. The length of the tube is L_z = 51 Å, and the radius is R = 15 Å. The distribution of charges is as follows. $x(i) = R \cos \varphi$, $y(i) = R \sin \varphi$, $z(i) = [(i - 1)/3 + 0.5]L/(n_q/3) + 10.0$, where $\varphi = 2\pi(i - 1)/3 + \mathrm{mod}(j,2)\pi/3$, and $j = (i - 1)/3$. L = 31 Å is the length of the charged part of the cylindrical tube.

Details of the Molecular Dynamics Model. To simulate electroosmotic driven flow, the system includes electrolyte and solid walls with discrete surface charges. In the simulation system, several key physical parameters determine the final simulation results such as the density of the surface charge and the density of the co-ions and the counterions. As we know, the simulation scale for a molecular dynamics model is very small, so it is unpractical to directly compare the MD model with the current experimental results. This produces the problem that it is difficult to select physical parameters from the experimental measurement results. Most previous work selected the initial parameters based on one constraint condition, that is, the simulation system should be always kept in electrical neutrality, which means the net charge of the solution equals the number of surface charges. However, it is still difficult to determine the number of the co-ions and the counterions from the only one constraint condition. For example, given a surface charge number of −10e, one can get several sets of the co-ion and counterion numbers to keep the system in neutrality, such as (−3e, +13e), (−5e, +15e), (−10e, +20e) etc. So, all previous work in the reported literature assumes the number of the co-ion and the counterion somewhat arbitrarily. To get the exact number of ions for a certain surface charge density and a certain bulk electrolyte concentration, a "sink−pump−sink" model was proposed in this letter as shown in Figure 1. In this model, only in the middle part, called the pump, surface charges are assigned on the solid wall. At the two ends of the tube, no surface charge is distributed on the solid wall. With periodical boundary conditions applied along the tube axis, the two end parts play the role as water sinks. The surface charge density is given at first. The final ion distribution is extracted from the simulation system as it reaches equilibrium.

Table 1. Parameters for Lennard-Jones Interaction

pair	σ/Å	ϵ/(kJ·mol^{-1})	pair	σ/Å	ϵ/(kJ·mol^{-1})
O−O	3.169	0.6502	Na^+−Na^+	2.583	0.4184
Na^+−O	2.876	0.5216	Cl^-−Cl^-	4.401	0.4184
Cl^-−O	3.785	0.5216	Na^+−Cl^-	3.87	0.4184
O−Ca^{2+}	3.019	0.5216	Ca^{2+}−Cl^-	3.635	0.4184

At the initial state, the model is kept in neutrality through setting the net charge number in the solution equal to the surface charge number. The sodium chloride solution is confined in the cylindrical nanopore and the co-ions and the counterions are randomly distributed in the solution. 1043 water molecules and 102 charged ions are included in the tube. Only in the pump part of 3.1 nm in length is the cylindrical wall distributed with elementary charges. The discretely distributed charges[16] are frozen to their original locations during the simulation. The number of the surface charge varies from −12 to -62e to investigate their effects on the ion distribution. The surface charge number of −62e corresponds to a surface charge density of about −0.34 C/m^2. Such a charge density can be considered as truly high. However, it is still possible in practical systems.[17] The numbers of the Na^+ and Cl^- ions in the system are chosen according to the surface charge density to maintain the electric neutrality of the system. MD simulations are performed with a modified TINKER 4.2[18] program package. The water is modeled using the SPC/E (extended simple point charge) model,[19] and the electrostatic interactions among ions, water molecules, and surface charges are modeled by the Ewald summation algorithm.[20] Lennard-Jones interaction parameters used in the calculation are listed in Table 1. The first 1 500 000 steps are used to equilibrate the simulation system. Once the system reaches equilibrium, the ion distribution and the solution density over the whole system can be obtained from the following 1 500 000 steps. In this model, the ion distribution is obtained from an equilibrated system through the atom diffusion process, so it is more reliable. After the ion distribution is obtained, an electric field is applied through the region of the pump. Another 1 500 000 steps are used to simulate the electroosmotic driven flow.

The wall is qualitatively like the hydrophilic surface of silica, and the interactions between the surface and the fluid molecules are also the same as reported in ref 16 using the Steele potential[21]

$$u_{wf}(r) = 2\pi\rho_w\epsilon_{wf}\sigma_{wf}{}^2\Delta\left[\frac{2}{5}\left(\frac{\sigma_{wf}}{R-r}\right)^{10} - \left(\frac{\sigma_{wf}}{R-r}\right)^4 - \left(\frac{\sigma_{wf}{}^4}{3\Delta(R-r+0.61\Delta)^3}\right)\right] \quad (1)$$

where $\rho_w = 42.76$ nm^{-3} and $\Delta = 2.709$ Å; σ_{wf} and ϵ_{wf} are obtained from bulk silica parameters as $\epsilon_w/k_B = 230$ K, $\sigma_w = 3.0$ Å and the fluid molecular parameters by Lorentz−Berthelot rules. R is the radius of the cylindrical tube and r is the distance of the solution particles from the center of the nanopore. The Newton's equations of motion are integrated using the velocity Verlet algorithm[22] with a time step of 2 fs. Berendsen thermostat[23] is used to keep the temperature at 298.0 K with a time constant of 0.1 ps. Only velocity components in the x and y directions are thermostated to not disturb the electroosmotic flow velocity profiles.

Continuum Theory in a Narrow Cylindrical Tube. Consider a steady-state electrolyte with ions continuously distributed in the whole cylindrical tube of radius R, the local electrostatic potential ψ across the tube can be described by the Poisson's equation in the cylindrical coordinate

$$\nabla^2\psi(r) = \frac{1}{r}\frac{d}{dr}\left(r\frac{d\psi}{dr}\right) = -\frac{\rho(r)}{\epsilon\epsilon_0} \quad (2)$$

where $\rho(r)$ is the excess charge density at a point of a distance, r, from the axis of the tube. ϵ is the permittivity of the fluid, which is assumed to be uniform, and ϵ_0 is the vacuum dielectric constant. Here $\epsilon = 81$ and $\epsilon_0 = 8.854 \times 10^{-12}$ C/V·m. The ion concentration in the solution can be expressed by the Boltzmann equation

$$n_i = n_{i0}\exp(-z_i e\psi/k_B T) \quad (3)$$

where n_i is the number of ion i in a unit volume and n_{i0} is the concentration at the tube center (where $\psi = 0$). z_i is the valence of ion i, e is the elementary charge (i.e., 1.6×10^{-19} C). k_B is the Boltzman constant, and T is the temperature of the medium. In monovalent electrolyte, the excess charge density can be written as

$$\rho(r) = \sum_i n_i z_i e = -2n_0 e\sinh\frac{e\psi}{k_B T} \quad (4)$$

If $e\psi/k_BT$ is small, then $\sinh e\psi/k_BT \approx e\psi/k_BT$, which is valid for $|\psi|$ up to 50 mV.[24] Setting $\kappa = (2n_0e^2/\epsilon\epsilon_0k_BT)^{1/2}$, where κ^{-1} is the so-called Debye length (electrical double layer thickness), then the Poisson−Boltzmann distribution equation has the form

$$\frac{1}{r}\frac{d}{dr}\left(r\frac{d\psi}{dr}\right) = \kappa^2\psi \quad (5)$$

The boundary conditions are that ψ is a constant at the center axis of the pore, $\psi|_{r=0} = 0$, and $\psi|_{r=R} = \psi_0$, where ψ_0 is the potential at the wall. Then, the solution of the Poisson equation is[24]

$$\psi(r) = \psi_0\frac{I_0(\kappa r)}{I_0(\kappa R)} \quad (6)$$

where I_0 is the zero-order modified Bessel function of the first kind. Equation 4 then becomes

$$\rho(r) = -\epsilon\epsilon_0\kappa^2\psi = -\epsilon\epsilon_0\kappa^2\psi_0\frac{I_0(\kappa r)}{I_0(\kappa R)} \quad (7)$$

Because the simulation system is neutral, the overall ionic charges should be equal to the total surface charges

$$\int_0^R \rho(r)\pi[(r+dr)^2 - r^2]L_s = n_s \quad (8)$$

where n_s is the number of the total surface charges. With a given n_s, substituting eq 7 into eq 8, the potential at the wall, ψ_0, can be obtained. Combining eq 3 and 6, the exact ion concentration from the Poisson−Boltzmann equation can be solved.

When the cylindrical tube is applied with an electric field along the axis direction, the Navier−Stokes equation of the motion for a Newtonian fluid is

$$\mu\frac{1}{r}\frac{d}{dr}\left(r\frac{dv_z}{dr}\right) - E_z\rho(r) = 0 \quad (9)$$

Here μ is the viscosity coefficient and equals 7.43×10^{-4} Pa·s, which is higher than the viscosity of 6.6×10^{-4} Pa·s as reported for the SPC/E water[25] because there are certain concentration of ions in the solution. Considering that the velocity at the wall is zero and there is no velocity gradient in the center of the tube, the boundary conditions are $v_z(R) = 0$ and $dv_z/dr|_{r=0} = 0$. From eq 9 and the boundary conditions, the electroosmotic flow velocity v_z can be solved as

$$v_z(r) = \frac{\epsilon\epsilon_0\psi_0}{\mu}E_z\left[1 - \frac{I_0(\kappa r)}{I_0(\kappa R)}\right] \quad (10)$$

Results of MD Simulations and Discussions. To investigate the effects of surface charges on ion distribution, a nanotube without any surface charge is also simulated as a comparison to the charged ones. Figure 2 and Figure 3a−c present the concentration profiles of the Na^+ and Cl^- ions and water molecules across the tube without and with different surface charges, respectively. When there is no surface charge on the wall, that is, the potential is zero at the wall, the distribution of the ions is in good agreement with the Poisson−Boltzmann results within the range from the tube center axis to 10.5 Å away as shown in Figure 2. An interesting finding is that there is no ion close to the tube surface in the MD simulations, which is different from the predicted results from the classical theory. There are two reasons for this discrepancy. First, each ion has an inherent size so that it cannot approach too close to the smooth wall. Second, the ions tend to stay away from the region close to the wall so as to not disturb the order of the packed water molecules.[16]

From Figure 3a−c, it can be seen that when the pump surface (the middle part of the nanotube) is charged, the densities of the counterions have concentration peaks at about 2 Å from the wall, and higher peaks can be observed in the

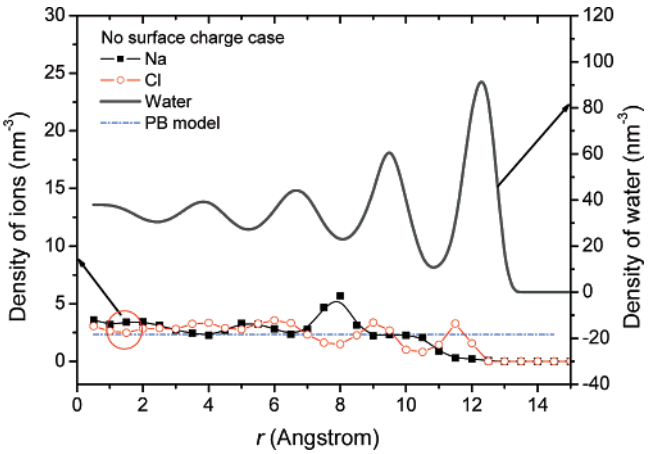

Figure 2. Ion and water density distribution in NaCl solutions along the radial direction in the nanotube without any surface charge.

tubes with larger numbers of surface charges. With the number of surface charges increasing from −22 to -62e, the sodium ion density increases from 10 to 25 ions/nm^3. However, even with the high surface charge of −62e in the nanotube, which corresponds to a charge density of −0.34 C/m^2 that is seldom true in practical engineering, charge inversion does not occur in Figure 3. For comparison, $CaCl_2$ solution is also simulated in the same nanotube with the same surface charge density as that in Figure 3c. The initial concentration of $CaCl_2$ is 1 M (Ca^{2+}) over the whole system and the results are shown in Figure 4. In this case, charge inversion can be clearly seen in the diffused layer, where the half concentration of co-ions is higher than the concentration of divalent counterions. The highly packed divalent counterions in the inner layer close to the surface of the nanotube repel counterions in the diffused layer. Therefore, more divalent counterions are accumulated in the center region of the nanotube. These simulation results do not support the observations of Qiao and Alura[8] and Besteman and co-workers[14] but agree with the recent experimental results[26,27] indicating that with the increase of the monovalent ion concentrations, the charge inversion observed in solutions of multivalent ions can be reduced or even canceled, clearly showing the screening effects of monovalent ions to charge inversion.

The ion concentrations can also be solved from the Poisson−Boltzmann equation. As presented in Figure 3a−c, the dashed curves labeled as PB model give the sodium ion distribution along the radial direction in the nanotube. In this case, instead of setting a constant charge on the surface, the boundary condition for eq 5 is set as $\psi(15.0) = \psi_0$, which means the potential on the nanotube surface is a constant. This is a routine selection for the boundary condition that is widely used in continuum theory. The problem is that the standard approach of applying boundary condition at the surface of the nanotube cannot fit the MD data well. Particularly, it cannot predict the peak location of the ion density along the radial direction near the wall. Note that the different ways of applying boundary conditions (constant number of surface charges for molecular dynamics

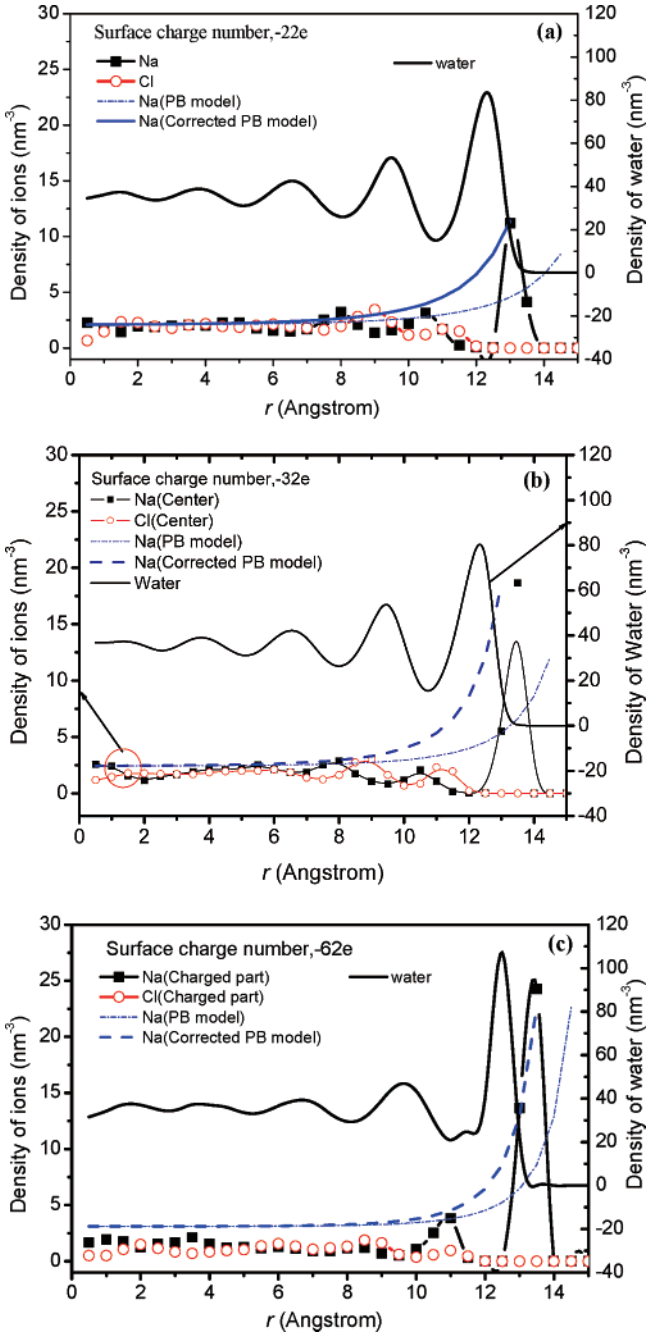

Figure 3. Ion and water density distribution in NaCl solutions along the radial direction in the middle section of the nanotube with different numbers of surface charges. The ion distribution in the two bulk regions is not shown here because the profiles are nearly the same as that the uncharged case in Figure 2. The densities of Cl^- ion predicted by the Poisson−Boltzmann equation are very small and not shown. (a) For −22e surface charges; (b) for −32e surface charges; and (c) for −62e surface charges.

simulation and constant surface potential for the Poisson−Boltzmann equation) used will not lead to the discrepancies between the results from the molecular dynamics simulation and the Poisson−Boltzmann equation. This is because the boundary condition for the Poisson−Boltzmann equation is based on the best fit to the molecular dynamics results. The value of the potential on the wall is adjusted to achieve the best fit for the results from the Poisson−Boltzmann equation

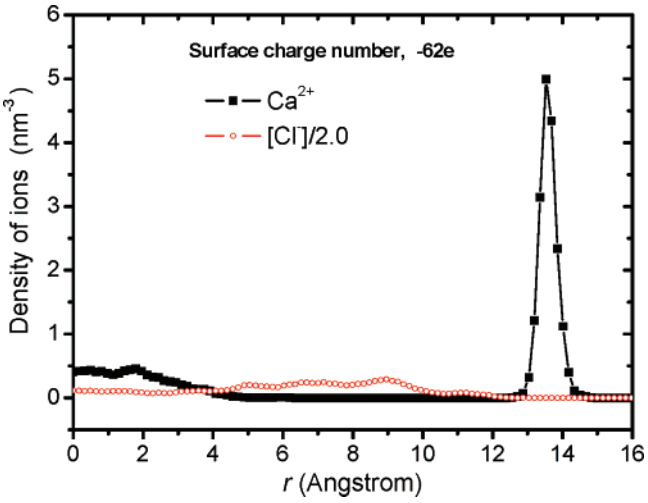

Figure 4. Ion distribution for 1.0 M $CaCl_2$ solutions confined in the nanotube with −62e surface charges. In this figure, the concentration of Cl^- is divided by 2.

to the molecular dynamics data so no other selection of the boundary condition for the PB equation can present better agreement.

To better compare the MD data with the predicted results from the PB theory, corrected boundary conditions for eq 5 have to be used, which are determined by the rule of the best fit with the MD data. In Figure 3, the corrected PB models correspond to different boundary conditions for eq 5, that is, $\psi(13.0) = \psi_0$ (for −12 and −32e) and $\psi(14.0) = \psi_0$ (for −62e). With the corrected boundary conditions, the predicted results from the PB model fit better with the MD data except deviations near the wall. Near the wall, the MD results demonstrate that there are a valley and a peak of the Na^+ ion concentration, while PB theory predicts that the concentration should decrease monotonically to its value in the tube center. In the valley, the concentration of Na^+ ion is close to zero, so the distribution of the ions can be described as discrete to some extent. The discrete nature of the ion distribution is caused by the size effects of the atoms, which cannot be captured by the continuum theory. Under the electrostatic action between the sodium ions and the negative surface charges, the Na^+ ions are very densely packed at the first peak. Meanwhile, with the increase of the Na^+ ions in the peak, the strong electrostatic repulsion among the ions make it difficult to accommodate more ions there. The maximum concentration is limited by the finite size of the ions and the force balance from different electrostatic interactions. Figure 3a−c demonstrates that the first peak of the ion distribution appears at the position of 1∼2 Å away from the solid wall. With the increase of the surface charge density, the distance between the first peak and the solid wall becomes smaller, which implies the attractive force on the counterions become stronger.

The charged part in the middle of the nanotube in Figure 1 is extracted after the system reaches steady state. The charged nanotube of 3.1 nm in length was simulated for another 3 ns to reequilibrate and was followed by a 3 ns production run. In this simulation, an extra electric field of 0.1 V/Å is applied to the nanotube to generate electroosmotic

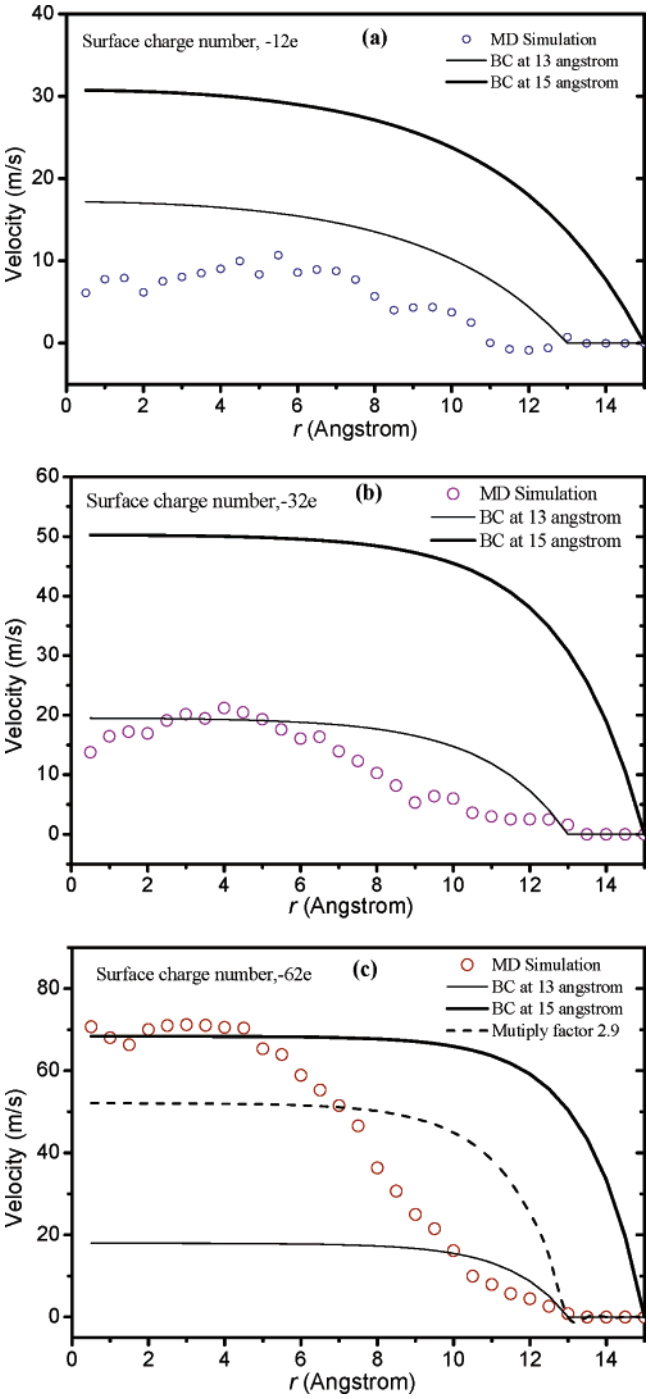

Figure 5. The electroosmotic flow velocity profiles for different surface charge numbers with an applied electric field of 0.1 V/Å. The figure shows both the MD simulation results and results from the Navier−Stokes equation with different boundary conditions. (a) −12e surface charges; (b) −32e surface charges; and (c) −62e surface charges.

flow. This high electric field is used to avoid relatively large thermal noise. The velocity profiles obtained are shown in Figure 5.

The comparison of continuum theory velocity profiles with the simulation results is given as follows. The basic equation of motion for the liquid in the nanotube is given by eq 10, and the solution is also shown in Figure 5. However, the continuum theory results for the surface charge number of −12 and −32e are much larger than the MD simulation results. On the basis of the distribution of water molecules in Figure 3, there are no particles within the first ∼1.5 Å from the wall, and the region of 1.5∼2.0 Å from the wall can be considered as the "stagnant layer" with an average velocity of zero. However, in continuum theory, the boundary condition for eq 10 is that the velocity at the wall is zero. Therefore, the location where the velocity is zero should be shifted to give a better fit to the MD simulation results, that is, $v_z(13.0) = 0$, and then eq 10 can be rewritten as

$$v_z(r) = \frac{\epsilon\epsilon_0\varphi_0}{\mu I_0(\kappa R)} E_z[I_0(\kappa R') - I_0(\kappa r)] \qquad (11)$$

where $R' = 13.0$ Å. The velocity profiles from eq 11 agree well with the MD simulation results in the central region of the nanotube for the −12 and −32e cases. The MD simulation velocity profiles are lower than the results of eq 11 in the area of 2∼10 Å away from the wall, which may be caused by the increased viscosity. The variation of the viscosity near the wall has been reported in many previous reports.[9−11] In Freund's simulations, the viscosity started rising at about 10 Å from the wall and could be six times larger than the bulk viscosity.[9] However, a comprehensive explanation for the dramatic increase in viscosity is not available yet. When the number of the surface charge is −62e, the continuum theory result from eq 11 still deviates significantly from the MD simulation velocity profile. The potential at the wall is about −71.5 mV and $\sinh e\psi_0/k_BT \approx 2.9 * e\psi_0/k_BT$ for the −62e case, that is, the excess charge density from eq 4 is underestimated. So the excess charge density is amplified by 2.9 times to give an approximate result. Then the solution from eq 11 is much closer to the MD simulation velocity profile as shown in Figure 5c. The velocity profiles of the MD simulation in the three cases are all related to the ion distribution in Figure 3. Although the counterions accumulate near the wall and a concentration peak occurs, they are dehydrated there and tightly adsorbed to the surface charges, which prevent the counterions from forming a directional motion. At the point of the concentration valley, the density of counterions is so low that the counterions there provide little driven force for the solution.

The reason that the Poisson−Boltzmann equation with corrected boundary condition can predict the velocity profiles in the center of the nanotube is that the velocity profile mainly depends on the Bessel function but the absolute magnitude of the velocity in the center of the nanotube relies on the boundary conditions. In fact, this is exactly the reason that the Navier−Stokes equation with the corrected boundary conditions can predict the velocity profiles well in the center of the nanotube, but fails near the wall. The corrected boundary condition helps to compensate for the high viscosity and molecular nature (layering effects near the surface) in the near wall region so the velocity profile in the center of the nanotube is acceptable but the high viscosity and layering effects in the near wall region cannot be reflected in the solution of the Navier−Stokes equation.

Conclusions. The ion distribution and electroosmotic flow in nanotubes with different surface charge densities have been investigated by MD simulation and continuum theory. Some conclusions that may be helpful to the design of nanofluidic devices are presented as follows:

(a) For the various cases of nanotubes with different surface charge densities, the Poisson−Boltzmann equation fails to predict the exact ion distribution. The primary reason is that the hypotheses for the Poisson−Boltzmann equation do not hold for fluid at nanoscale in which the dimension of the nanotube is comparable to the Debye length, for example, both water molecules and ions form layering structures across the nanotube. Additionally, the distribution of water in nanotubes is significantly different for different surface charge densities. There are more counterions attracted when the surface carries more elementary charges and the water concentration close to the wall is also higher because of the hydration of the ions.

(b) When an electric field is applied in the direction tangential to the surface, the fluid will be dragged by the charged ions and electroosmotic flow is generated. With modified boundary conditions, the Navier−Stokes equation based on the continuum assumption can predict the velocity profiles well in the center of the nanotube, but fails near the wall because of the increasing liquid viscosity and the neglecting of the molecular nature of interactions. It can be inferred from the simulations that with the same external electric field, increasing the surface charge density will speed up the electroosmotic flow.

(c) In this letter, two regions in the nanotube without surface charges are introduced to play the role of water sinks. This model is more realistic in simulating the ion distribution in nanoscale channels. Simulation results demonstrate that charge inversion does not occur even at high surface charge densities for monovalent ion solutions.

Acknowledgment. G.W. gratefully acknowledges the guidance and suggestions from Dr. XiongWu Wu of the National Institute of Health and Professor A Bródka of University of Silesia of Poland. This work was supported by the National Basic Research Program of China (2006CB-300404), National Natural Science Foundation of China (Grant 50475077). Z.N. acknowledges the financial support from the High Technology Program of China (2006AA04-Z351). D.L. acknowledges the support of the U.S. National Science Foundation (CBET 0643583).

References

(1) Stone, H. A.; Stroock, A. D.; Ajdari, A. *Ann. Rev. Fluid Mech.* **2004**, *36*, 381−411
(2) Chen, C. H.; Santiago, J. G. *J. Microelectromech. Syst.* **2002**, *11* (6), 672−683.
(3) Kuo, T. C.; Cannon, D. M., Jr.; Chen, Y. *Anal. Chem.* **2003**, *75*, 1861−1867.
(4) Reyes, D. R.; Iossifidis, D.; Auroux, P. A.; Manz, A. *Anal. Chem.* **2002**, *74* (12), 2623−2636.
(5) Qiao, R.; Aluru, N. R. *Int. J. Numer. Meth. Eng.* **2003**, *56*, 1023−1050.
(6) Crozier, P. S.; Henderson, D.; Rowley, R. L. *Biophys. J.* **2001**, *81*, 3077−3089.
(7) Guo, Z.; Zhao, T. S.; Shi, Y. *J. Chem. Phys.* **2005**, *122*, 144907, 1−10
(8) Qiao, R.; Aluru, N. R. *Phys. Rev. Lett.* **2004**, *92*, 198301, 1−4.
(9) Freund, J. B. *J. Chem. Phys.* **2002**, *116*, 2194−2200.
(10) Qiao, R.; Aluru, N. R. *J. Chem. Phys.* **2003**, *118* (10), 4692−4701.
(11) Qiao, R.; Aluru, N. R. *Int. J. Multiscale Comput. Eng.* **2004**, *2* (2), 173−188.
(12) Zhu, W.; Singer, S. J.; Zheng, Z. *Phys. Rev. E* **2005**, *71*, 041501, 1−12
(13) Greberg, H.; Kjellander, R. *J. Chem. Phys.* **1998**, *108* (7), 2940−2953.
(14) Besteman, K.; Zevenbergen, M. A. G.; Lemay, S. G. *Phys. Rev. E* **2005**, *72* (6), 061501, 1−9.
(15) Thompason, A. P. *J. Chem. Phys.* **2003**, *119* (14), 7503−7511
(16) Cui, S. T.; Cochran, H. D. *J. Chem. Phys.* **2002**, *117* (12), 5850−5854.
(17) Poppe, H.; Cifuentes, A.; Kok, W. *Anal. Chem.* **1996**, *68* (5), 888−893.
(18) Ponder, J. W. *TINKER−Software tools for molecular design*, User's Guide for Version 4.2; Washington University School of Medicine: St. Louis, MO, 2004.
(19) Berendsen, H. J. C.; Grigera, J. R.; Straatsma, T. P. *J. Phys. Chem.* **1987**, *91*, 6269−6271.
(20) Brodka, A.; Sliwinski, P. *J. Chem. Phys.* **2004**, *120* (12), 5518−5523.
(21) Steele, W. A. *Surf. Sci.* **1973**, *36*, 317−352
(22) Allen, M. P.; Tildesley, D. J. *Computer Simulation of Liquids*; Oxford University Press: New York, 1987; pp 78−82
(23) Berendsen, H. J. C.; Postma, J. P. M.; van Gunsteren, W. F. *J. Chem. Phys.* **1984**, *81* (8), 3684−3690.
(24) Rice, C. L.; Whitehead, R. *J. Phys. Chem.* **1965**, *69* (11), 4017−4024.
(25) Balasubramanian, S.; Mundy, C. J.; Klein, M. L. *J. Chem. Phys.* **1996**, *105* (24), 11190−11195.
(26) Besteman, K.; Zevenbergen, M. A. G.; Heering, H. A.; Lemay, S. G. *Phys. Rev. Lett.* **2004**, *93*, 170802.
(27) Frank, H. J. H.; Derek, S.; Besteman, K.; Lemay, S. G.; Dekker, C. *Phys. Rev. Lett.* **2006**, *96*, 224502.

NL0718566